DJS Vol. 49 (1) (2024) – pp.112-130 ISSN: 1012-5965

Delta Journal of Science
Available online at
https://djs.journals.ekb.eg/

Research Article

GEOLOGY

Egyptian Silica Sand-Based Materials for Supercapacitor Applications: Towards Sustainability

Rawan A. Elshewhy[1*], Mona M. Fawzy[2], Sally M. Youssry[3], Saad G. Mohamed[4], Mohamed M. Hamdy[1*]

[1]Geology Department, Faculty of Science, Tanta University, Tanta 31527, Egypt.
[2]Physical Dressing Department, Nuclear Materials Authority, P.O. Box 530, Cairo, Egypt.
[3]Chemestry Department, Faculty of Science, Tanta University, Tanta 31527, Egypt
[4]Mining and Metallurgy Engineering Department, Tabbin Institute for Metallurgical Studies (TIMS), Tabbin, Helwan 109, Cairo 11421, Egypt.

***Corresponding Authors:** R. Elshewhy **e-mail:** Rwanelshwehy86@gmail.com
M. Hamdy mohamed.hamdy@science.tanta.edu.eg

Received: 23/9/2024 **Accepted:** 14/10/2024

KEY WORDS

Wadi Qena silica sand; Quartz mineral; Mineralogical characterization; Physical beneficiation; Electrochemical performance for Supercapacitors

ABSTRACT

Natural geological materials-based supercapacitors have attracted a lot of attention in research because of the global energy problem and the growing campaign against carbon emissions. Exploiting mineral raw materials containing Si-oxide as an alternative to synthesized oxides for supercapacitors provides sustainability values. To this end, quartz mineral concentrate sourced from Wadi Qena silica sand in the Eastern Desert of Egypt was investigated as a viable supercapacitor electrode material. With an average of 98% mass, quartz mineral (SiO_2) was purified (as confirmed by XRD, FT-IR, and EDX analysis) through a series of physical processes, including attrition scrubbing and gravity separation. Employing a three-electrode configuration with 6 M KOH electrolyte, the working electrode has been constructed by slurrying active mineral material, conductive additive (super P) and polyvinlidene difluoride as a binding agent in dimethyl formamide in a proportion of 7:2:1. Electrical impedance spectroscopy (EIS), galvanostatic charging and discharging, and cyclic voltammetry were used to evaluate the electrochemical performance. Concentrated quartz demonstrated substantial specific capacitance/capacity of 40.17 F g^{-1} at 1 mvs^{-1}. EIS showed improved charge transfer and ion diffusion. Quartz concentrated from silica sand shows promise for supercapacitor applications. The availability of silica sand in Egypt, combined with low-cost beneficiation processes, highlights the potential for supercapacitor applications. This study emphasizes the significance of additional investigation into similar geological resources in Egypt, focusing on their value for the renewable energy industry and contributing to global sustainable development goals.

Introduction

Recent advancements in energy storage systems, particularly supercapacitors, have focused on providing affordable solutions for storing electricity during off-peak times for future use. This research aims to boost the viability of renewable energy sources **(Scalfi et al., 2021; Nikitina, et al., 2024)** . Since the early 2000s, many nations, especially those prioritizing sustainability, have turned to renewable energy as a result of dwindling fossil fuel reserves, disruptions in fossil fuel availability caused by events like the Covid-19 pandemic and the war between Ukraine and Russia **(Asen et al., 2019)**, and the environmental effects of emissions of greenhouse gases from the use of fossil fuel.

In Egypt, the rising demand for renewable energy is driven by both population growth and economic progress. In its efforts to move away from fossil fuels, Egypt is also dedicated to the United Nations Framework Convention on Climate Change (UNFCCC) **(Asen et al., 2019)** and supports the recommendations from COP26 **(Backović et al., 2024)**, COP27 **(Lienard, 2022)**, and COP28 **(Locke et al., 2023)**.

Because SiO_2 has a large theoretical capacity and the potential to improve its electrochemical properties, it is widely used as a material for electrodes in supercapacitors **(Baig et al., 2021; Sajjad, 2021)**. However, SiO_2 alone is an insulator with poor electrical conductivity, so it is often used in combination with conductive additives. In the composite, material consists of SiO_2, carbon black, and polyvinylidene fluoride (PVDF). SiO_2 provides structural stability and high surface area, while carbon black enhances electrical conductivity **(Sajjad, 2021)**. PVDF acts as a binder, ensuring that the active materials are well-integrated and maintain structural integrity during operation. This combination leverages the strengths of each component to improve the overall performance of the supercapacitor.

Wadi Qena in the Eastern Desert of Egypt holds 257.8 million tons of silica sand with high content of silicon dioxide (SiO_2) **(Guo and Henderson, 2019)**, yet Egypt remains heavily reliant on imports for its mineral and chemical needs, which constitutes a significant portion of its total imports. To capitalize on its natural resources and align with Egypt's Vision 2030 focused on sustainable development, improving quality of life, and enhancing global competitiveness **(Elgohary, 2022)**. It is essential to

utilize local resources like SiO_2 for supercapacitor production. The current study aims to conduct an integrated assessment of Wadi Qena silica sand for the preparation of electrode materials for supercapacitors, taking into account geological occurrence, the most cost-effective and environmentally friendly physical methods of extracting SiO_2, and electrochemical performance.

SiO_2 Deposits in Wadi Qena

The geological section with silica sand deposits in the northern part of Wadi Qena lies 20 km south of the El-Sheikh Fadl–Ras Gharib Road **(Wilmsen, and Nagm, 2013; Said, 2017; Tawfik, et al., 2017)**, at coordinates 27° 57' 57" N, 32° 30' 58" E **(Fig. 1).** The Wadi Qena silica sand deposits are primarily located within the Naqus Formation.

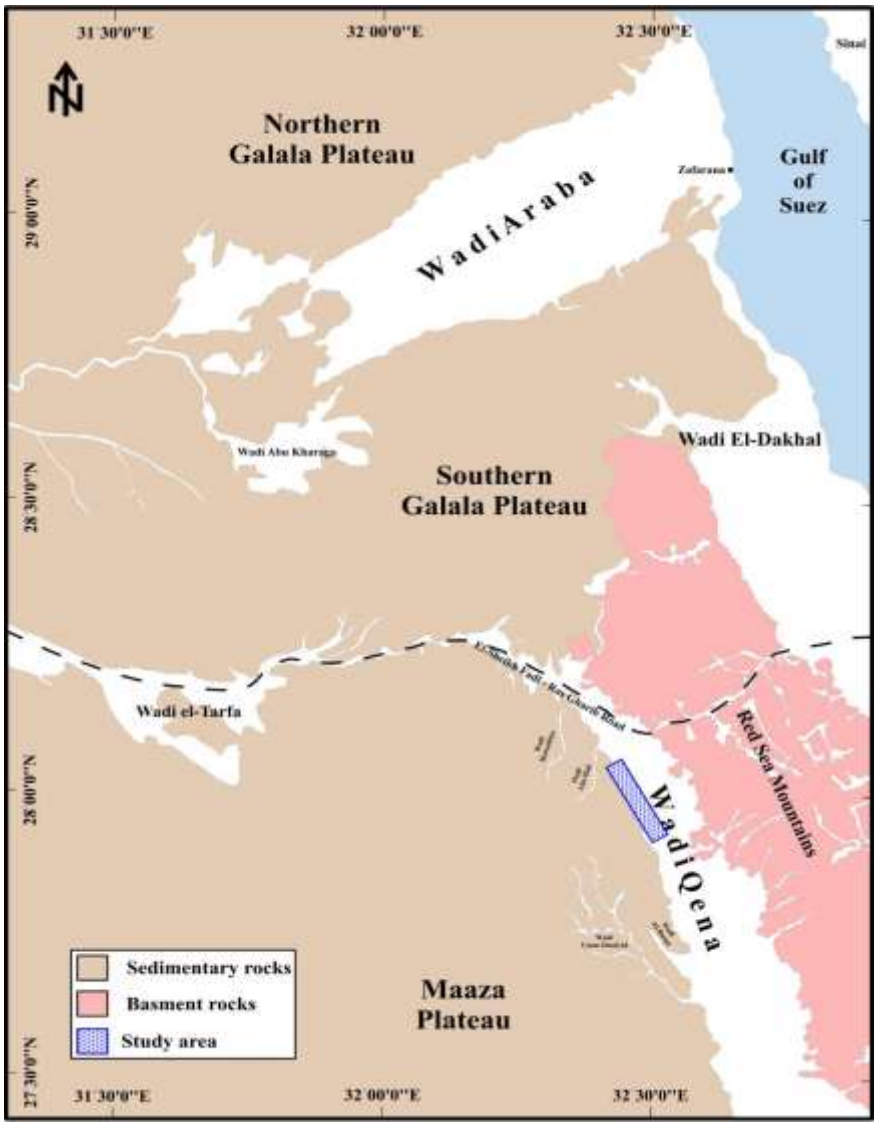

Fig. (1): Geological map of the studied area, North Wadi Qena, Eastern Desert, Egypt.

The Naqus Formation, part of the Lower Paleozoic strata, features well-sorted quartz grains within its fluvial sandstones, resulting from the weathering and erosion of quartz-rich rocks. In the Galala Formation, which is about 120 meters thick, silica sand is found in thin to medium-grained sandstone layers and shaly siltstones, also formed through the weathering of quartz-rich rocks **(Tawfik et al., 2017) (Fig. 2)**. These deposits illustrate Wadi Qena's economic significance for mineral extraction, as well as the area's extensive geological history, which includes complicated weathering, sedimentary, and hydrothermal processes.

Fig. (2): Field photograph shows white silica sand deposits within Naqus Formation, North Wadi Qena, Eastern Desert, Egypt.

Fluvial, tabular, cross-bedded Lower Cretaceous sandstones mostly composed of ferruginous quartz arenite, quartz greywacke, and quartz arenite comprise the Naqus Formation **(Tawfik et al., 2017)**. The kaolinite proportion decreases with every stage of its cyclic sedimentation processes. Varying depositional circumstances are suggested by kaolinitic nodules that expand across into the sandstones. The main component of kaolin in the Naqus Formation is kaolinite, which produced when mica and feldspar weathered chemically in conditions of high humidity. With silica development, the sandstones were primarily composed of sorted well quartz grains that range in size from angled to round. The erosion and weathering of quartz-rich rocks,

which were subsequently carried and deposited in river environments, forms these quartz grains.

Methods of Study

A technological raw silica sample from Wadi Qena, weighing approximately 50 kg, was used as the primary sample for this study. The technological sample was produced from ten samples taken from various surface outcrops and trenches in the areas where quarries are produced. Kaolinitic, white to yellowish-brown, medium- to coarse-grained, semi-compacted to loose, and weakly cemented characteristics distinguish out the collected samples. The sample was first weighed, thoroughly blended, and separated into representative fractions using John's riffle splitter for characterization and beneficiation procedures, with a single fraction kept as a reference.

Physical beneficiation techniques were applied to concentrate and separate quartz and kaolinite from the Wadi Qena silica sand as it is one of the easiest and cheapest methods compared to chemical and thermal methods. Physical upgrading procedures don't use chemicals or high temperatures, which pollute the environment, making them ecologically friendly methods. They are also less expensive because they don't require heat energy or chemicals **(Nzeh et al., 2009).**

Granulometric analysis of a representative portion of the sample was performed using a set of sieves with aperture dimensions of 1.0, 0.5, 0.250, 0.125, and 0.063 mm (ASTM codes) and a mechanical sieve shaker. This analysis identified the particle size distribution as well as the particles' relative weights.

A separate portion of the Wadi Qena silica sand was subjected to an attrition scrubbing experiment, and the scrubbed sand product was analyzed through sieving. Comparative analysis was conducted between the original and scrubbed samples. Additionally, approximately 100 grams of the original sample were tested for heavy mineral content using bromoform ($CHBr_3$, specific gravity of 2.89) through heavy liquid separation.

Mineralogical identification and morphological characterization of the Wadi Qena raw sample were conducted using scanning electron microscope (SEM) linked with an energy dispersive spectrometer (EDS), X-ray diffraction (XRD) and Fourier Transform Infrared spectroscopy (FT-IR). SEM-EDS confirmed the structural and compositional characteristics, while XRD analysis was conducted on the raw material and separated silica using the APD 2000 PRO X-Ray diffractometer with CuKα radiation. FT-IR analysis of the purified silica was performed with

the Cary 630 FT-IR spectrometer, covering a spectral range from 400 to 4000 cm^{-1}. Monomineralic grains were prepared by handpicking under an Olympus stereo binocular microscope.

Energy dispersive X-ray fluorescence (ED-XRF- Axios Advanced Sequential XRF Spectrometer) was used to determine major and trace element contents in the original sample, each size fraction, and the final products after beneficiation. After being ground to a powder (less than 75 μm) in an agate mortar, powder samples were heated to 1000°C for two hours to measure the loss on ignition (L.O.I.). For major elements, the threshold limit was 20 ppm, while for trace elements, it was 2 ppm. These analyses were conducted at the laboratories of the Egyptian Nuclear Materials Authority.

The silica sand purification was conducted in two steps. In the first step, attrition scrubbing was utilized to separate kaolinite, which was then classified using a hydrocyclone. In the second stage, heavy mineral concentration was achieved by a wet-gravity separation using a Wilfley shaking table No. 13.

Purified SiO_2 mineral is prepared and loaded onto a nickel foam electrode for electrochemical measurements. The cyclic voltammetry (CV) technique is used at different scan rates, the galvanostatic charging and discharging (GCD) technique is used at different current densities, and the electrochemical impedance (EIS) is measured at different frequencies. Electrochemical measurements were performed at the Tabbin Institute for Metallurgical Studies in Cairo using a Voltalab 40 PGZ 301 electrochemical station (Radiometer Analytical, France). The electrochemical studies were carried out utilizing a three-electrode layout with 6M KOH solution as the electrolyte. The working electrode was made by combining the active material (SiO_2), conducting additives (Super P), and poly (vinylidene difluoride) (PVDF) as a binder in dimethylformamide (DMF) at the weight proportion of 7:2:1. The slurry was then applied to nickel foam supplied by MTI, South Korea. The nickel foam (1cm × 3cm × 1.6 mm) was cleaned using sonication in acetone for 30 minutes, treated with 3 M HCl for 10 minutes, and finally rinsed with deionized water (DIW) and ethanol to eliminate contaminants and oxides from the surface. It was then dried at 70°C. Before doing electrochemical tests, the electrode being used was soaked in 6 M KOH for 12 hours to enable full ion penetration into the active material.

Results and Discussion

Characterization of Silica Sand Raw Material

Granulometric study was the first step in characterizing Wadi Qena raw silica sand in order to comprehend the fractional mass distribution. A representative sample weighing about 175 g was subjected to granulometric analysis after being moved to the top sieve in the organized set of sieves and sieved for 15 minutes. There were six size fractions that were generated: (-0.063mm), (-0.125+0.063), (-0.25+ 0.125), (-0.5+0.25), (-1+0.5), and (+1 mm). The range of -0.5 + 0.063 mm was found to include around 77.5% mass of raw silica sand, being close to the % of the allowable weight (80%) in British Standard Specifications (BS 2975: 1988) of high quality sand, which is suitable for physical beneficiation to produce high-grade white sand. The fine fraction smaller than 0.063 mm, or 4% mass, is used as feed for kaolinite separation, whereas the remaining 18.5% of the mass is bigger than 0.5 mm and should be rejected as oversized and containing impurities.

The chemical assays of the raw silica sand and the fractionated products after attrition scrubbing are shown in Table (1). The SiO_2 grade of the head bulk sample was high, at 94.29%, and the other impurity elements were assayed as alumina (3.7% $A1_2O_3$), titinia (0.4% TiO_2), lime (0.25% CaO), and iron oxide (0.102% Fe_2O_3).

Table (1): XRF composition of Wadi Qena raw silica sand in comparison with its products from attrition scrubbing

Elemental oxide	Raw Sand	-0.5+0.063 mm	-0.063 mm
	Wt. %		
SiO_2	94.290	96.17	89.71
Al_2O_3	3.700	2.45	6.5
Cao	0.245	0.196	0.275
TiO_2	0.398	0.264	0.91
Fe_2O_3	0.102	0.08	0.32
P_2O_5	0.084	0.077	0.09
K_2O	0.030	0.023	0.023
CoO	0.002	0.0022	0.0039
ZnO	0.003	0.0017	0.0089
CuO	0.002	0.0021	0.0018
V_2O_5	0.010	0.016	0.0619
PbO	0.001	0.00081	0.0037
NiO	0.003	-	0.0025
Cr_2O_3	0.003	-	0.0039
L.O.I	1.120	0.72	2.09

The morphological description for raw sand reveals the presence of different shapes of sand grains. Figure (3) depicts some spherical grains, while others are angular or elongated.

Together with a thorough microscopic inspection, the XRF and XRD analysis results demonstrate three essential minerals—quartz (~89.88 mass %), feldspar (~1.46% mass %), and kaolinite (~8.03% mass %)—make up Wadi Qena silica sand.

Wadi Qena silica sand Beneficiation

Chemical and mineralogical analysis of the Wadi Qena silica sand sample revealed that kaolinite was the most

abundant impurity found with the sand, as well as traces of several heavy minerals like ilmenite and rutile. Therefore the beneficiation procedures were as follows: attrition scrubbing followed by a hydro-cyclone classifier to separate the kaolinite content. We conducted sieving analyses to remove material larger than 0.5mm and smaller than 45 µm. Heavy minerals were separated using a shaking table as wet gravity separation technique. Various factors were examined throughout the operations to optimize conditions.

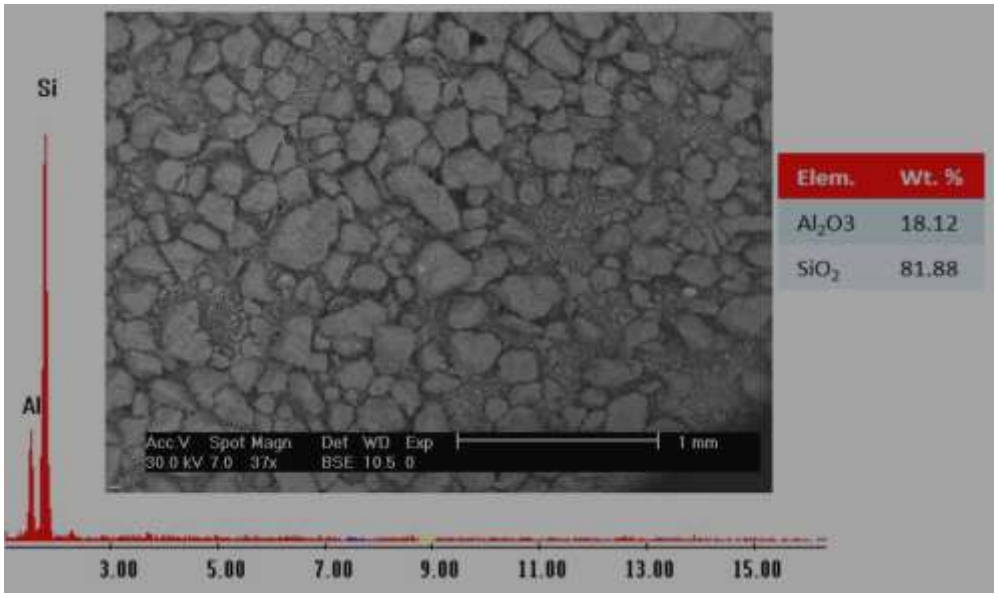

Fig. (3): Back-scattered electron (BSE) image and corresponding EDS spectrum for Wadi Qena raw silica sand.

Attrition scrubbing

The simplest method for treating the sand grains' surface to get rid of clays and certain oxide coatings that stick to the grain surface by pressing the sand grains together is known as attrition scrubbing. A mechanical stirrer was used to conduct an attrition test on a Wadi Qena silica sand sample. At first, the samples were washed without any stirring. After that, the samples were cleaned for around 20 minutes at 1800 rpm using distilled water. The undersize-screen fraction was fed into a 2" and 1" Mozley hydrocyclone classifier at the optimal pressure settings to yield a product with a mesh size of -25 microns and reject the very fine sand that followed. The byproduct kaolinite was recovered after complete drying. Afterwards the cleaned sand sample was weighed and examined with SEM-EDS. The scrubbed sand underwent grain size analysis and was compared to the size distribution analyses for the head sample (Fig. 4). The optical microscopic

examination revealed that the sand was cleaner and the kaolinite concentration was lower. Although the proportion of silica in the scrubbed sample increased, as shown by the EDS spectra (Fig. 5), the Al, Ca, and K% dropped. However, these elements are still present in trace amounts, meaning that additional scrubbing will be necessary to eliminate them.

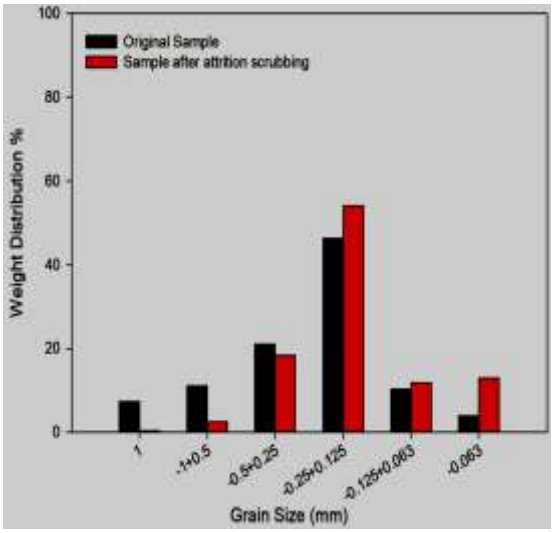

Fig. (4): Histogram comparing granulometric analyses of Wadi Qena silica sand before and after attrition cleaning.

Shaking Table Concentration

A shaking table (Model: WILFLEY TABLE NO.13) was employed to increase silica sand grade whilst eliminating heavy minerals. To create high-grade silica sand, a roughing concentration phase was first performed, and then the produced silica sand underwent to an additional cleaning concentration step to minimize the heavy minerals as much as feasible. The following operating conditions were optimized for the roughing and washing stages using a shaking table: 134 g/min feeding rate, 14 L/min water flow rate, 1.5 cm stork length, 9° tilt angle for the rougher step, and 140 g/min feed rate, 17.5 L/min water flow rate, 2 cm stork length, and 11° tilt angle for the cleaning step.

A representative head bulk sample was separated without fractionation, followed by a sample that had been size fractionated and divided into three fractions (-0.5 + 0.25mm), (-0.25 + 0.125mm), and (-0.125mm). The separation process for the head bulk sample was unsuccessful because of particle size differences. The final products formed during the attrition scrubbing, rougher, and cleaning processes for the Wadi Qena silica sand sample were collected, dried, weighed, and elementally analyzed by XRF spectrometry, with results compared to the head sample and displayed in Table (2). The silica assay rises from 94.29% in the head sample to 96.89% after attrition, then to 97.25% after the rougher stage, and finally to 98.71% after the cleaning step. On the contrary, Al_2O_3 reduces from 3.7% to 0.7%, TiO_2 from approximately 0.4% to 0.1% and Fe_2O_3 from 0.10% to 0.04%. The presence of these uncommon impurities in silica sand may improve its performance as an electrode material for

supercapacitors **(e.g., Lukatskaya et al., 2013; Dar et al., 2024)**.

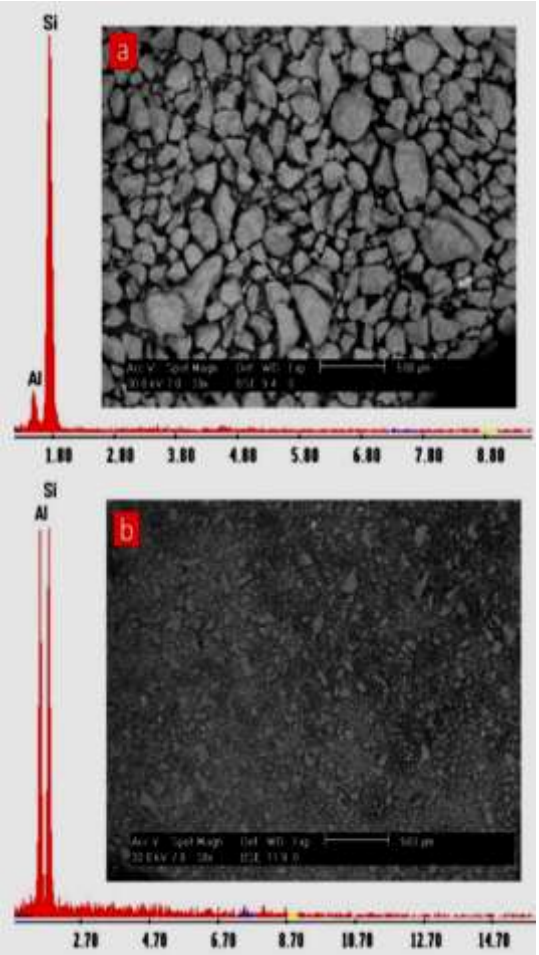

Fig. (5): BSE image and corresponding EDS spectrum for Wadi Qena silica sand products after attrition scrubbing; a. sand size product (-0.5+0.063 mm), b. clay size fraction (-0.063 mm).

Mineralogical Characterization of the Separated Silica

The separated silica from Wadi Qena silica sand underwent XRF Table (2) and XRD (Fig. 6) examination. Figure (6) shows the acquired XRD diffractograms that were compared to the ICDD diffraction results. Several Bragg diffraction peaks, along with their corresponding crystallographic planes, confirm that the concentrate consists solely of kaolin and silica sand, respectively. Its diffraction (2θ=20.9° (100), 2θ=26.6° (101), 2θ=36.5° (110), 2θ = 50.1° (112)) planes of quartz. The FTIR analysis of the separated silica shows an absorption band at 1084.25 cm^{-1} (Fig. 7). The asymmetric stretching vibrations of the Si-O-Si bonds in quartz structure cause this band. The absorption bands at 800-850 cm^{-1} is attribute to Si-O bending vibrations, often referred to as the δ(Si-O-Si) bending mode. The absorption band at 788.09 cm^{-1} is also related to Si-O bending vibrations, particularly the γ(Si-O-Si) bending mode. The absorption band at 463.22 cm-^{1} demonstrates Si-O-Si bending vibrations in the quartz crystal lattice. The absorption peak at 3434.9 cm^{-1} in SiO_2 indicates stretching vibrations of hydroxyl (OH) groups caused by environmental exposure **(Iwasawa., 1986; Bonneviot and Kaliaguine, 1995; Larkin, 2017)**. The patterns of the EDAX (Fig. 8) confirm that the separated silica is mainly composed of quartz. This is consistent with the mineralogical composition estimated using the XRD analysis.

Table (2): XRF composition of the Wadi Qena silica after purification.

Elemental oxide	Raw sand	Sand after attrition	Sand after rougher step	Sand after cleaning step
	Wt. %			
SiO_2	94.290	96.89	97.25	98.71
Al_2O_3	3.700	1.84	1.77	0.7
Cao	0.245	0.31	0.172	0.168
TiO_2	0.398	0.34	0.134	0.135
Fe_2O_3	0.102	0.058	0.054	0.042
P_2O_5	0.084	0.074	0.073	0.062
K_2O	0.030	0.029	0.043	0.059
CoO	0.002	0.0017	0.0024	0.0027
ZnO	0.003	0.0024	0.0016	0.0024
CuO	0.002	0.0018	0.0016	0.0012
V_2O_5	0.010	0.0225	0.0073	-
PbO	0.001	0.0009	0.0012	0.00086
NiO	0.003	-	-	-
Cr_2O_3	0.003	-	-	-
L.O.I	1.120	0.43	0.49	0.11

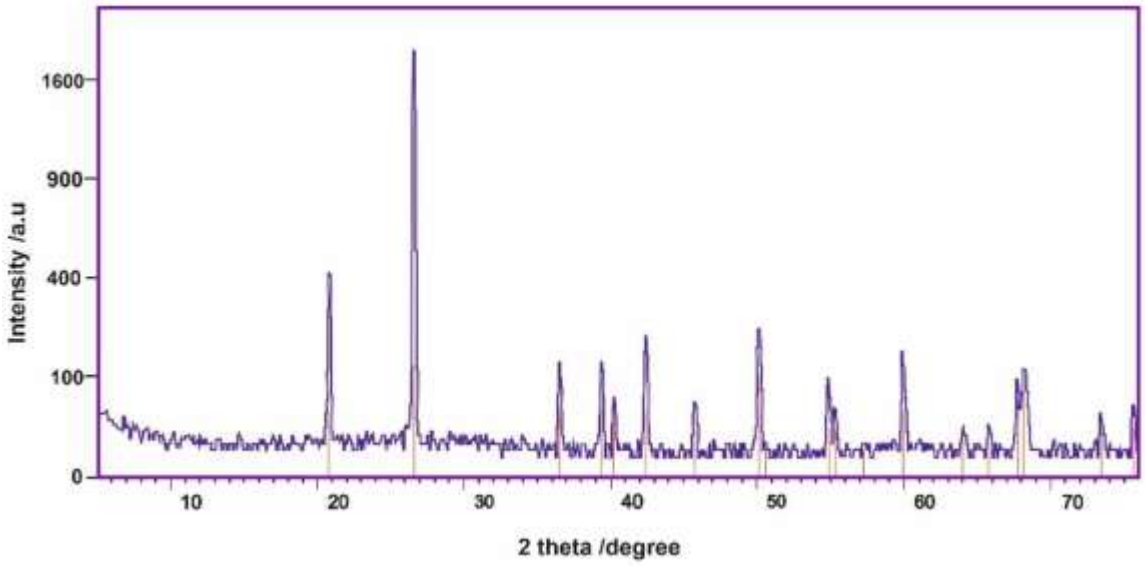

Fig. (6): XRD of separated silica.

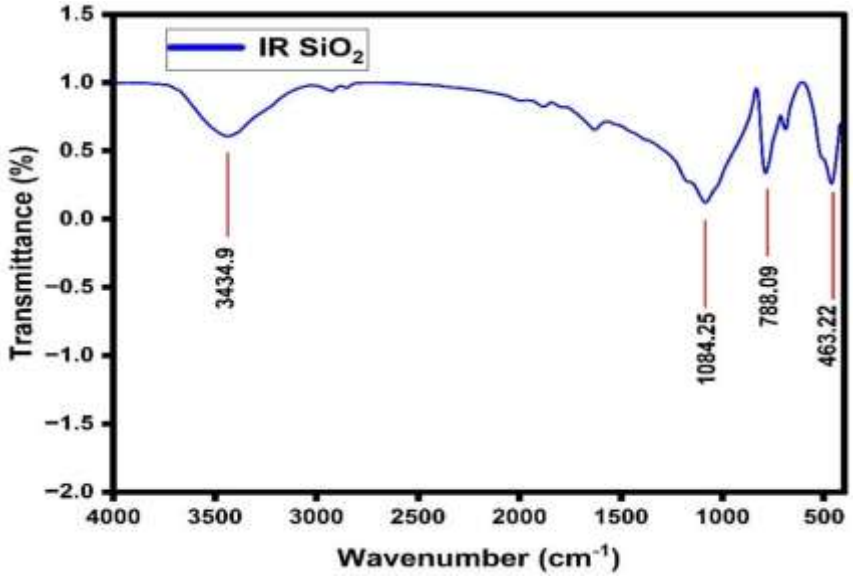

Fig. (7): FT-IR of separated silica.

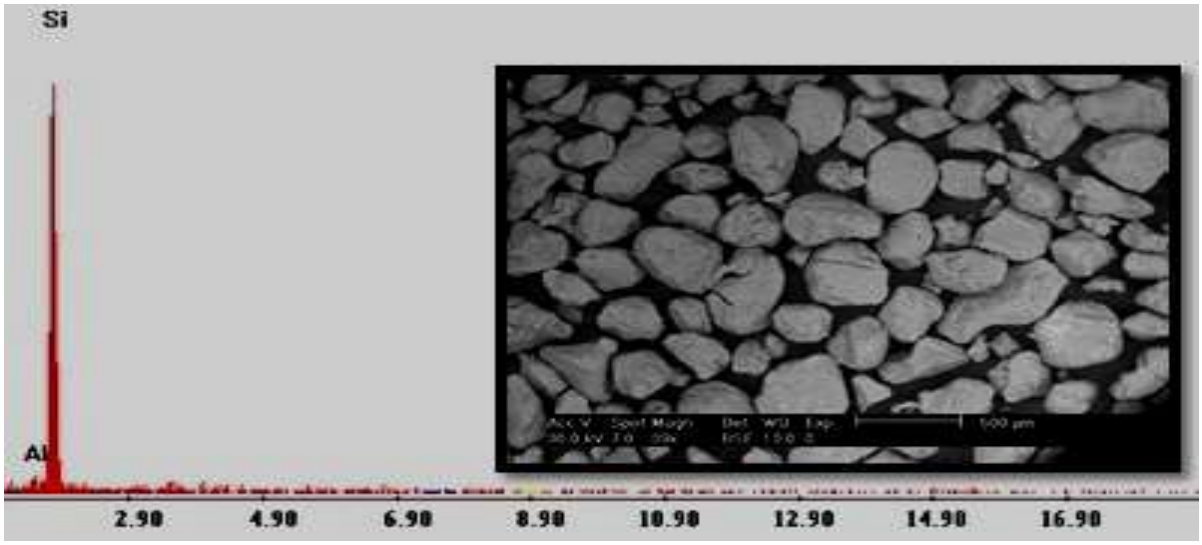

Fig. (8): EDXA of separated silica.

Electrochemical measurements

The electrochemical behavior of the separated silica was assessed using an electrochemical measurement station (Voltalab 40 PGZ 301, Radiometer Analytical, France) through cyclic voltammetry (CV), galvanostatic charging and discharging (GCD), and electrochemical impedance spectroscopy (EIS). CVs were logged within a potential window ranging from 0 to 0.6 V (vs. Hg/HgO) at scan rates ranging from 5 to 100 mV s^{-1}. GCD measurements were done at current densities ranging from 1 to 5 A g^{-1} within a voltage window of 0 to 0.55 V.

EIS measurements were made using Nyquist plots in the frequency range of 100 kHz to 0.01 Hz. The GCD data were used to determine specific capacitance (Csp, F g^{-1}) and capacity (Cs, $C.g^{-1}$) using the following equations **(Mohamed et al., 2018; Shao et al., 2018; Noori et al., 2019)**:

$$\mathbf{Csp} = \frac{2\,I \int V\,dt}{m\,V^2}\ \mathbf{(F.g^{-1})}$$

$$\mathbf{C_s} = \frac{2\,I \int V\,dt}{m\,V}\ \mathbf{(C.g^{-1})}$$

where I is the discharging current (A), Δt is the discharging time (s), ΔV is the discharging potential range (V), and m is the active material's mass (g).

Using three electrodes in 6 M KOH, CV, GCD, and EIS tests were made to assess the electrochemical efficacy of silica as an active electrode material for supercapacitors. The silica CV curves at various sweep rates, ranging from 5 to 100 mV s^{-1}, are displayed in Fig. (9a) in a potential window of 0 to 0.6 V. The curves show a non-capacitive Faradic-redox character, with prominent Faradaic reactions and redox couples, which are characteristic of an electrode with a battery-like signature.

A redox reaction involving a composite slurry of SiO_2, carbon black, and polyvinylidene fluoride (PVDF) in a 7:2:1 ratio, deposited on nickel foam, can be understood by examining the electrochemical activity during cyclic voltammetry (CV) analysis. In this configuration, SiO_2 may contribute to pseudo-capacitive behavior by facilitating surface redox reactions with electrolyte ions. Carbon black enhances electrical conductivity, aiding efficient charge transfer, while nickel foam acts as a current collector, supporting the overall redox activity of the electrode.

During CV measurements, distinct redox peaks, rather than the rectangular shape typical of pure electric double-layer capacitance, are observed. These peaks indicate the presence of Faradaic reactions, where reversible electron transfer processes occur. SiO_2, along with possible nickel oxide formation on the foam, participates in oxidation and reduction reactions, thereby contributing to energy storage through redox mechanisms. These peaks in the CV curve indicate active redox behavior, which is essential for raising the supercapacitor's total capacitance and performance.

The SiO_2 CV plot on nickel foam sheds light on the composite's electrochemical characteristics. The x-axis represents the applied potential (E) versus a Hg/HgO reference electrode, while the y-axis represents current density (A/g), which indicates the electrochemical reactions occurring within the material. The multiple curves, recorded at changed scan rates (5, 30, 50, 80, and 100 mV/s),

are used to assess the material's response to varying rates of potential change.

The plot includes distinct anodic (oxidation) and cathodic (reduction) peaks, demonstrating the redox processes present in the system. Though SiO_2 is typically non-conductive, it becomes electrochemically active when incorporated into the conductive nickel foam matrix. The nickel foam, with its high surface area and porosity, enhances electron transfer and provides more active sites for redox reactions, leading to increased current densities.

The rise in peak current with increasing scan rates suggests that the electrochemical process is diffusion-controlled. This indicates that at higher scan rates, the electroactive species' diffusion to the electrode surface becomes a limiting factor. Additionally, the broadening of peaks at higher scan rates implies some degree of capacitive behavior, suggesting that the system not only relies on Faradaic processes but also stores charge electrostatically, as is common in supercapacitors.

Overall, the configuration of the CV curves shows that this composite material may give a respectable amount of energy storage capacity because of the double-layer capacitance and redox processes combined with quick electron and ion movement, as well as high power. The synergistic combination of SiO_2, carbon black, and nickel foam enables efficient charge storage and transfer, making it a promising material for supercapacitor applications.

CV is used to study the redox behavior, capacitance, and stability of supercapacitors. Measure specific capacitance (Cs) of minerals sample was derived from CV curves using the equation:

$$C_s = \frac{\int IdV}{m \nu \Delta V}$$

where the capacitance (C) of a supercapacitor can be calculated using the integrated area (A) of the CV curve, the voltage window (V), the scan rate (νs), and the mass of active materials (m). Significant redox peaks were always seen in a 6 M KOH electrolyte at different potential scan speeds, which ranged from 5 to 100 mV s^{-1} (Fig. 9a). This demonstrates the hybrid supercapacitor's predominant battery-like reaction after assembly. The SiO_2 electrode's electrochemical processes are regulated by the migration of hydroxide ions from the electrolyte to the electrode surface, as demonstrated by the linear relationship between the square root of the rate of scanning and the peak current density of anodic/cathodic reactions within the 5 to 100 mV s^{-1} range. GCD experiments done within a potential range of 0 to 0.55 V at varying current density show almost flat charging and

discharging plateaus at stable voltage stages, coupled to substantial Faradaic-redox couple reactions, as shown in Fig. (9b), comparable with previous CV measurements.

The specific capacitances were calculated from the CV curves , showing that the calculated specific capacitances were 51.9, 40.2, 37.3, 34.6, and 33.3 F/g at scan speed of 5, 30, 50, 80, and 100 mv s^{-1}, in that order. The specific capacitances were also calculated from the GCD discharge curves. At current density of 1, 2, 3, 4, and 5 A g^{-1}, the specific capacitance of 40.5, 36.09, 36.08, 35.9, and 34.6 F/g were computed. These correspond to specific capacity of 22.2, 19.85, 19.84, 19.78, and 19.05 C g^{-1}.

SiO_2's cycle stability was assessed using continuous charging and discharging cycling at a constant current charge density of 4 A g^{-1}. Figure (9c) shows that SiO_2 retains 99.3% of its original capacitance after 1,000 cycles and 94.5% after 3,000 cycles. Wadi Qena purified silica's long-term stability and performance in supercapacitor applications can be attributed to a variety of factors, such as: nanoporous structure, which allows for effective transportation of ions and charge retention **(Salanne et al., 2016)**; mechanical strength, which prevents damage during cycling **(Huang et al., 2022)**; chemical durability, which is achieved by silica's ability to inhibit corrosion and deterioration from the electrolyte **(Du et al., 2024)**; hybrid design, which enhances silica with conducive materials—particularly titanium—for improved electron transport (**Raj and Prasanth, 2018)**; and at last, low inner resistance, which ensures effective electricity storage with minimal heat development **(Ibraheem et al., 2022)**.

Electrochemical impedance spectroscopy (EIS) was also conducted to assess the transport of charges and ion diffusion. Figure (9 d) shows the Nyquist plots for the silica electrode prior to and following 3,000 charge/discharge cycles. Each EIS spectrum includes a semicircle in the high frequency zone and a straight line in the low frequency zone. The slope of the straight line in the low frequency zone corresponds to ion diffusion resistance, whereas the diameter of the semicircle in the area of high frequencies indicates charging resistance. The curve's intersection with the real axis in the high-frequency region represents the equivalent series resistance (ESR), which includes the electrolyte resistance, the intrinsic resistance of the active electrode material, and the contact resistance at the boundary between the active material and current collector. Initially, the value

of ESR for the studied silica electrode is 1.8 Ohm.

Before initiating charge-discharge cycles, EIS data shows low charge transfer and solution resistance, indicating efficient electrochemical performance. After 3000 cycles, while there is an increase in resistance about 0.8 Ohms, it remains relatively small. This suggests that although some degradation or changes have occurred in the supercapacitor's materials or interface, the overall performance has been well-maintained. The relatively small increase in resistance indicates that the supercapacitor remains effective with only minor changes to its electrochemical properties.

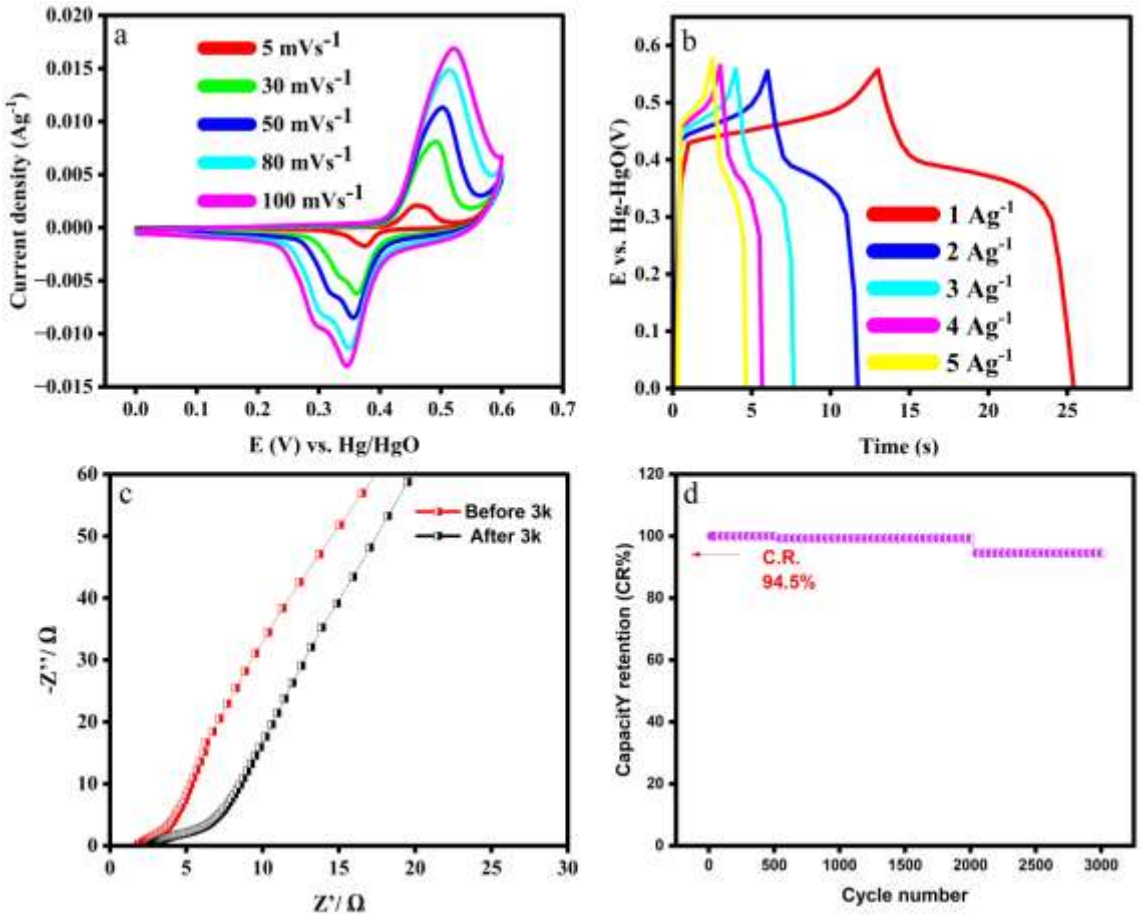

Fig. (9): (a) CV of Silica, (b) CD of silica, (c) EIS before and after 3000 cycles, and (d) stability of silica.

Conclusion

This study explores the potential of quartz mineral concentrate from Lower Paleozoic alluvial kaolinitic silica sand of Wadi Qena (Eastern Desert, Egypt) as an electrode material for supercapacitors. The global focus on energy sustainability and reducing carbon emissions has spurred interest in natural geological materials, including Si-oxide minerals, as alternatives to synthetic compounds. Quartz concentrates with 98% SiO_2, purified through attrition scrubbing and gravity separation was assessed for its

electrochemical performance in supercapacitors applying a three-electrode system with a KOH electrolyte. The mineral showed promising results, achieving a specific capacitance of 40.17 F g^{-1}.

Quartz's structure, paired with carbon black for conductivity and PVDF as binding agent, enhanced the material's electrochemical properties. The study highlights the availability of significant silica deposits in Egypt, particularly in Wadi Qena, which holds around 257.8 million tons of SiO_2. The low-cost beneficiation methods used, along with the abundance of silica sand, underscore its potential for contributing to Egypt's renewable energy sector and reducing reliance on imports. The research aligns with Egypt's Vision 2030, promoting local resource utilization, economic growth, and sustainability.

References

Asen, P., Haghighi, M., Shahrokhian, S., & Taghavinia, N. (2019). One step synthesis of SnS2-SnO2 nano-heterostructured as an electrode material for supercapacitor applications. *J. Alloys Compd.*, 782: 38-50.

Backović, N., Jakšić, M., & Ilić, B. (2024). The Impact of Energy on Climate and Economic Stability: Forecast for Serbia. *J. Cent. Bank. Theory Pract.*, 13(1): 199-222.

Baig, M. M., Pervaiz, E., Azad, M., Jahan, Z., Niazi, M. B. K., & Baig, S. M. (2021). NiFe2O4/SiO2 nanostructures as a potential electrode material for high rated supercapacitors. *Ceram. Int.*, 47(9) : 12557-12566.

Bandel, K., Kuss, J., & Malchus, N. (1987). The sediments of Wadi Qena (Eastern Desert, Egypt). *J.Afr.Earth Sci*., 6(4) : 427-455.

Bonneviot, L., & Kaliaguine, S. (Eds.). (1995). Zeolites: a refined tool for designing catalytic sites. Elsevier.

Dar, M. A., Majid, S. R., Satgunam, M., Siva, C., Ansari, S., Arusalan, P., & Ahamed, S. R. (2024). Advancements in Supercapacitor electrodes and perspectives for future energy storage technologies. *Int.J.Hydrogen Energy*, 70: 10-28.

Du, J., Hou, X., Zhu, W., Zhou, H., She, X., Yang, Q., & Tsou, C. (2024). Mechanically Robust and Electrically Conductive Hybrid Hydrogel Electrolyte Enabled by Simultaneous Dual In Situ Sol-Gel Technique and Free Radical Copolymerization. *Macromol.Rapid Commun.*, 2400404.

Elgohary, E. (2022). The role of digital transformation in sustainable development in Egypt. *Int. J. Inform. Media Commun.*, 4(1) : 71-106.

Guo, C., & Henderson, R. A. (2019). Evidence of a crustal source, independent of primary melt generation, for pluton-related W-Sn mineralization in the Dongpo orefield, Hunan Province, South China. *Sn-W-Critical Metals & Associated Magmatic Systems*, 41.

Huang, J., Han, S., Zhu, J., Wu, Q., Chen, H., Chen, A., Zhang, J., Huang, B., Yang, X. & Guan, L. (2022). Mechanically stable all flexible supercapacitors with fracture and fatigue resistance under harsh temperatures. *Adv.Funct.Mater.*, 32(35) : p.2205708.

Ibraheem, S., Yasin, G., Iqbal, R., Saleem, A., Nguyen, T. A., & Ibrahim, S.

(2022). Silicon-based nanomaterials for energy storage. In *Silicon-Based Hybrid Nanoparticles* (pp. 103-124). Elsevier.

Iwasawa, Y. (Ed.). (1985). *Tailored metal catalysts* (Vol. 7). Springer Science & Business Media.

Klitzsch, E., Groeschke, M., & Herrmann-Degen, W. (2017). Wadi Qena: Paleozoic and pre-campanian cretaceous strata. In *The Geology of Egypt* (pp. 321-327). Routledge.

Larkin, P. (2017). Infrared and Raman spectroscopy: principles and spectral interpretation. Elsevier.

Lienard, C. (2022). COP27 in Egypt.

Locke, J., Dsilva, J., & Zarmukhambetova, S. (2023). Decarbonization strategies in the UAE built environment: An evidence-based analysis using COP26 and COP27 recommendations. *Sustain.*, 15(15): 11603.

Lukatskaya, M.R., Mashtalir, O., Ren, C.E., Dall'Agnese, Y., Rozier, P., Taberna, P.L., Naguib, M., Simon, P., Barsoum, M.W. & Gogotsi, Y. (2013). Cation intercalation and high volumetric capacitance of two-dimensional titanium carbide. *Sci.*, 341(6153): 1502-1505.

Mohamed, S. G., Attia, S. Y., Barakat, Y. F., Hassan, H. H., & Zoubi, W. A. (2018). Hydrothermal synthesis of α-MnS nanoflakes@ nitrogen and sulfur Co-doped rGO for high-performance hybrid supercapacitor. *ChemistrySelect*, 3(22): 6061-6072.

Nikitina, A. A., Lavrentev, F. V., Yurova, V. Y., Piarnits, D. Y., Volkova, O. O., Skorb, E. V., & Shchukin, D. G. (2024). Layered nanomaterials for renewable energy generation and storage. *Mater. Adv.*, 5(2) : 394-408.

Noori, A., El-Kady, M. F., Rahmanifar, M. S., Kaner, R. B., & Mousavi, M. F. (2019). Towards establishing standard performance metrics for batteries, supercapacitors and beyond. *Chem.Soc.Rev.*, 48(5) : 1272-1341.

Nzeh, N. S., Popoola, P., Okanigbe, D., Adeosun, S., & Adeleke, A. (2023). Physical beneficiation of heavy minerals–Part 1: A state of the art literature review on gravity concentration techniques. *Heliyon*, 9(8).

Raj, C. C., & Prasanth, R. (2018). Advent of TiO_2 nanotubes as supercapacitor electrode. J. Electrochem. *Soc.*, 165(9), E345.

Said, R. (2017). The Geology of Egypt.: Routledge.

Salanne, M., Rotenberg, B., Naoi, K., Kaneko, K., Taberna, P.L., Grey, C.P., Dunn, B. & Simon, P. (2016). Efficient storage mechanisms for building better supercapacitors. *Nat. Energy*, 1(6) : 1-10.

Sajjad, M. (2021). Recent advances in SiO2 based composite electrodes for supercapacitor applications. J. Inorg. Organomet. Poly m. Mater., 31(8): 3221-3239.

Scalfi, L., Salanne, M., & Rotenberg, B. (2021). Molecular simulation of electrode-solution interfaces. *Annu. Rev. Phys.Chem.*, 72(1): 189-212.

Shao, Y., El-Kady, M.F., Sun, J., Li, Y., Zhang, Q., Zhu, M., Wang, H., Dunn, B. & Kaner, R.B. (2018). Design and mechanisms of asymmetric supercapacitors. *Chem. Rev.*, 118(18): 9233-9280.

Tawfik, H. A., Ghandour, I. M., Maejima, W., Armstrong-Altrin, J. S., & Abdel-Hameed, A. M. T. (2017). Petrography and geochemistry of the siliciclastic Araba Formation (Cambrian), east Sinai, Egypt:

implications for provenance, tectonic setting and source weathering. *Geol. Mag.*, 154(1): 1-23.

Wilmsen, M., & Nagm, E. (2013). Sequence stratigraphy of the lower Upper Cretaceous (Upper Cenomanian–Turonian) of the Eastern Desert, Egypt. *Newsl. Stratigr.*, 46(1): 23-46.

مواد من رمل السليكا المصري لتطبيقات المكثفات الفائقة :نحو الاستدامه

روان عبداللطيف الشويحي[١]، منى محمد فوزي[٢]، سالي محمد يسري[٣]، سعد جمعه محمد[٤]، محمد محمود حمدي[١]

[١]قسم الجيولوجيا- كلية العلوم- جامعة طنطا- طنطا ٣١٥٢٧- مصر
[٢]قسم تركيز الخامات الفيزيائى- هيئة المواد النووية- القاهرة - مصر
[٣]قسم الكيمياء- كلية العلوم- جامعة طنطا- طنطا ٣١٥٢٧ - مصر
[٤]قسم هندسة التعدين والمناجم- معهد التبين للدراسات المعدنية- حلوان - مصر

أدى التركيز العالمي على استدامة الطاقة والحد من انبعاثات الكربون إلى تحفيز الاهتمام بالمواد الجيولوجية الطبيعية، بما في ذلك معادن أكسيد السيليكون، كبدائل للمركبات الاصطناعية لاستخدامها في صناعة مخزنات الطاقة المتجددة. تستكشف الدراسة الحالية إمكانية استخدام ركاز معدن الكوارتز، والمؤكد تركيبة بتحليل حيود الاشعة السينية (XRD) وامتصاص الاشعة تحت الحمراء (FTIR) وتحليل الأشعة السينية المشتتة للطاقة (EDXA) وتحليل تفلور الاشعة السينية (XRF) من رمال السليكا الكاولينيتيه الغرينيه كمواد اقطاب للمكثفات الفائقة.

تتواجد الرمال محل الدراسة بتكوين الناقوس ذو عمر الباليوزوي السفلي في وادي قنا (الصحراء الشرقية، مصر). تم تنقية الرمال المستخدمة لتحتوي على ٩٨% SiO_2 والذي تم تأكيده بتحليل تفلور الاشعة السينية (XRF)، من خلال تنقية الاستنزاف والفصل بالجاذبية. بقياس الأداء الكهروكيميائي للسليكا المنقاه كمواد اقطاب في تطبيقات المكثفات فائقة السعة للتخزين للطاقة التي تطبق نظامًا ثلاثي الأقطاب مع إلكتروليت KOH وجد ان السعة المحددة قدرت ب ٤٠.١٧ فاراد/جرام. تم قياس التوصيلية الكهروكيميائية وأداء نقل الأيونات للمكثفات الفائقة باستخدام التحليل الطيفي للمقاومة الكهروكيميائية (EIS) باستخدام مخطط نيكويست لأقطاب الكوارتز حيث اظهر قيم ESR تبلغ ١.٨أوم. وكما ان النسبة المئوية للاحتفاظ بالسعة قدرت ب ٩٩.٣% عند ١٠٠٠ دوره وأصبحت ٩٤.٥% بعد ٣٠٠٠ دوره مما يضمن أداءً جيدًا في تخزين وتوصيل الطاقة على المدى الطويل. وقد أوضحت النتائج ان إلكترود الكوارتز المقترن بأسود الكربون للتوصيل وPVDF كعامل ربط، قد بين خواص كهروكيميائية أفضل.

وتسلط الدراسة الضوء على توافر رواسب كبيرة من السليكا في مصر، خاصة في وادي قنا، الذي يحتوي على حوالي ٢٥٧.٨ مليون طن من SiO_2 كما تبين ان طرق تركيزه منخفضة التكلفة وصديقة للبيئة، إلى جانب خواصها الكهروكيميائية الجيده مما يشير ا الي قدرة مساهمة هذه الرواسب السليكية في قطاع الطاقة المتجددة في مصر وتقليل الاعتماد على الواردات. مما يتوافق مع رؤية مصر ٢٠٣٠، لتعزيز استخدام الموارد المحلية، والنمو الاقتصادي، والاستدامة.